Journal of Molecular Modeling (2020) 26: 331
https://doi.org/10.1007/s00894-020-04591-2

ORIGINAL PAPER

Halogen bonds and other noncovalent interactions in the crystal structures of trans-1,2-diiodo alkenes: an ab initio and QTAIM study

Yongna Yuan[1] · Matthew J. L. Mills[2] · Fuyang Li[1] · Yuhong Du[1] · Jiaxuan Wei[1] · Wei Su[1]

Received: 6 June 2020 / Accepted: 27 October 2020 / Published online: 4 November 2020

Abstract

A series of interatomic interactions interpretable as halogen bonds involving I…I, I…O, and I…C(π), as well as the noncovalent interactions I…H and O…O, were observed in the crystal structures of trans-1,2-diiodoolefins dimers according to ab initio calculations and the quantum theory of "atoms in molecules" (QTAIM) method. The interplay between each type of halogen bond and other noncovalent interactions was studied systematically in terms of bond length, electrostatic potential, and interaction energy, which are calculated via ab initio methods at the B3LYP-D3/6-311++G(d,p) and B3LYP-D3/def2-TZVP levels of theory. Characteristics and nature of the halogen bonds and other noncovalent interactions, including the topological properties of the electron density, the charge transfer, and their strengthening or weakening, were analyzed by means of both QTAIM and "natural bond order" (NBO). These computational methods provide additional insight into observed intermolecular interactions and are utilized to explain the differences seen in the crystal structures.

Keywords Halogen bonding · *Noncovalent interaction* · ab initio calculation · Quantum theory of atoms in molecules · Topological properties

Introduction

Halogen bonds have recently been extensively studied as they play an essential role in medicinal chemistry [1, 2], molecular recognition [3], material science [4, 5], and crystal engineering [6–8]. Halogen bonds are noncovalent interactions between an electrophilic region of a halogen and a nucleophile [9, 10]. These interactions actually cover a range from very weak to fairly strong depending on the nature of the halogen, its environment, and the nature of the negative site. Halogen bonds can schematically be depicted R–X···Y, where X is a halogen (typically I, Br, Cl, and rarely F), and Y is defined as the halogen bond donor [11, 12]. X acts as an electron acceptor for the interaction, whereas Y is typically an electron-rich O, N, S, or Y–donor functional group (e.g., π–electron systems or aromatic surfaces). A halogen atom may be covalently bound to one or several atoms and can additionally form one or several halogen bonds simultaneously [9, 13, 14].

Halogen bonds have similarities with hydrogen bonds and involve the same mechanisms [15]. In 2008, Metrangolo et al. summarized the similarities and differences between halogen bonding and hydrogen bonding complexes [6]. Kirk et al. investigated the competition between hydrogen bonding and halogen bonding for the (Y = Cl, Br, I, At)/halogenabenzene/NH_3 systems and concluded that hydrogen bonding has an advantage when the halogen is Cl, while halogen bonds tend to be formed when the halogen atom Y = I [16]. Halogen bonds have been observed in crystal structures containing halogen atoms [17]. Due to their geometric properties, halogen bonds are considered efficient tools in designing the structures of crystals [6, 18]. The concept of halogen bonds in crystal engineering attracts increasing attention as they can be pivotal in the stability of crystals [19, 20].

Although halogen bonding was first observed two centuries ago [11], the fundamentals of its nature and its potential applications in crystal engineering have remained unexplored

Supplementary Information The online version contains supplementary material available at https://doi.org/10.1007/s00894-020-04591-2.

✉ Yongna Yuan
yuanyn@lzu.edu.cn

[1] School of Information Science & Engineering, Lanzhou University, No.222 South Tianshui Road, Lanzhou 730000, China

[2] 3M Corporate Research Analytical Laboratory, Saint Paul, MN 55114, USA

until recently. In most cases reported in the literature, halogen bonds were studied in cocrystals between two different compounds, one of which being the halogen bond donor and the other is the acceptor [17, 21]. On the basis of computational studies, this type of interaction was shown to predominantly originate from charge transfer and electrostatics [22–24]. Later, the interaction was also found to possess polarization and dispersion contributions. In 2014, Deepa et al. [25] carried out a theoretical study of a series of organic crystal structures containing various halogen bonds and found the strongest halogen bonds involved iodine as both halogen bond donor and acceptor. In the following year, Koskinen et al. [26] carried out a detailed study of unexpectedly strong I^+…S halogen bonds in $[I(2\text{-imidazolidinethione})_2]^+$ with the results supporting the coordinative nature of the halogen bond.

Furthermore, topological properties, vibrational frequencies, interaction energies, and charge transfer in halogen bond–containing systems have been studied using both Bader's quantum theory of atoms in molecules (QTAIM) [27] and Weinhold's "natural bond orbital NBO" methods. A series of important studies are through QTAIM theory [28–31]. Clark et al. [32] calculated the electrostatic potential of the series of molecules CF_3X (X = F, Cl, Br, and I) and found that the three unshared pairs of electrons produced a belt of negative electrostatic potential around the central region of the X atom (except for F), leaving the outermost region positive, which designated the "σ-hole." They also discovered that the strength of the σ-hole depends on the nature of the halogen atom. The more polarizable and the lower the electronegativity of the halogen atom, the more positive the σ-hole. Thus, the interaction strength of halogen bonds increases in the order of F < Cl < Br < I. It is the σ-hole that allows the halogen atom to form a halogen bond with a Lewis base [33] and that makes the A...X-R angle tend towards a linear configuration [15]. In 2010, Zeng et al. [34] comparatively analyzed the properties of halogen bonds and hydrogen bonds by QTAIM calculations and concluded that the two interactions were coincident in topological properties. In the following year, they analyzed halogen bonds between sulfides and dihalogen molecules and found that electrostatic interactions played an important role in these halogen bonds [35]. Grabowski [36] calculated the QTAIM characteristics of halogen bonds, dihalogen bonds, and halogen-hydride bonds. In 2018, Bauzá et al. [37] analyzed the interplay between π-hole and lone pair···π/X-H···π interactions through QTAIM calculations. In 2019, Benito et al. [38] first reported the cocrystallization of an adenine derivative which acts as a halogen bond acceptor; the calculations were carried out via DFT calculations and the QTAIM method. In 2020, Wzgarda-Raj et al. [39] investigated several observed types of halogen bonding interactions in a series of cocrystals in detail based on QTAIM. In addition to the traditional halogen bonds, Domagała et al. [40] built a model of a double (+/−)-charge-assisted halogen bridge for a set of quinuclidine-like cation derivatives and anions; these charged fragments were observed to form strong halogen bonding complexes, with interaction energies high as 100 kcal/mol.

In this work, calculations carried out on new crystal structures of trans-1,2-diiodoolefins are reported, including nine monomers and nine dimers. These crystal structures were previously synthesized by Hettstedt et al. [41] in 2015 (see Fig. 1). The purpose of this study is to investigate the characteristics and properties of halogen bonds (i.e., I…I, I…O, and I…C(π), where C(π) can be aromatic, aliphatic, or acetylenic π-systems) and other noncovalent interactions such as I…H and O…O observed in these crystal structures.

Computational methods

Data for halogen bonds observed in crystal structures of trans-1,2-diiodoolefins reported by Hettstedt et al. [41] have been used as references for quantum chemical calculations to analyze noncovalent interactions. The structures of monomers and dimers were obtained from the Cambridge Crystal Structure Database (CCSD). Geometry optimization, molecular electrostatic potential, and interaction energy calculations were carried out using the Gaussian09 program package [42–45]. The DFT-D3 method, which is recommended in studying noncovalent interactions [46–49], was applied to the monomer and dimer optimizations. Both Kolář et al. [50] and Bauzá et al. [51] verified that the B3LYP-D3 method

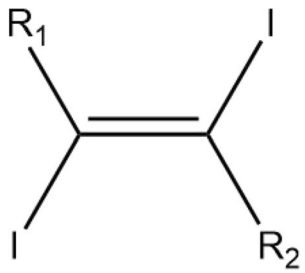

(1) $R_1 = R_2 = Ph$
(2) $R_1 = Ph$, $R_2 = Me$
(3) $R_1 = Ph$, $R_2 = H$
(4) $R_1 = Ph$, $R_2 = CH_2OH$
(5) $R_1 = Ph$, $R_2 = CO_2Me$
(6) $R_1 = Ph$, $R_2 = CO_2Et$
(7) $R_1 = Ph$, $R_2 = CH(COEt)_2$
(8) $R_1 = R_2 = CO_2Me$

Fig. 1 1,2-Diiodoolefines that have been studied in this work

combined with the "def2" basis set series can be used to successfully examine halogen bonds and the properties of σ-holes. Therefore, the B3LYP-D3/6-311++G(d,p) and B3LYP-D3/def2-TZVP levels of theory were used to optimize the structures of monomers. Frequency calculations were run to be sure that the geometry was a potential energy minimum (no negative frequencies were obtained). The keyword "counterpoise" was used for the calculations of corrected interaction energies (ΔE(AB)) including the inherent basis set superposition error (BSSE) [52] according to Eq. (1).

$$\Delta E(\mathrm{AB}) = E(\mathrm{A,B}) - \{E(\mathrm{A}) + E(\mathrm{B})\} + \mathrm{BSSE} \quad (1)$$

Here, E(AB) is the total energy of dimer AB and E(A) and E(B) are the energies of monomers A and B, respectively.

The electrostatic potential on the molecular surfaces of all monomers was analyzed in order to gain insight into the nature and directionality of the halogen bond interactions being considered herein. The electrostatic potentials were considered to be an outer contour of the electron density, and were cut off at the 0.001 au (electrons/bohr^{-3}) surface, as proposed by Bader et al. [53]. The most positive value of the potentials (the local maximum) is referred to as $V_{\mathrm{S,\ max}}$. Natural bond orbital (NBO) calculations were performed using the NBO 3.1 program [54] as implemented in Gaussian09. The QTAIM theory was applied to find critical points and these were analyzed in terms of electron density and the Laplacian. The topological properties at the bond critical points (BCPs) of halogen bonds were computed with the program-AIMALL 2000 [55].

Results and discussion

Monomers

Geometries

In the work reported in ref. [41], *trans* isomers were obtained for all systems but one: acetal 7, for which a mixture of *cis* (7a) and *trans* (7b) derivatives were formed in the synthetic process. Therefore, there are in total nine monomers reported on in this study. All of their geometries were optimized at the B3LYP-D3/6-311++G(d,p) and B3LYP-D3/def2-TZVP levels of theory. Figure 2 shows the nine trans-1,2-diiodoolefin structures optimized at the B3LYP-D3/6-311++G(d,p) level of theory. The C=C bond lengths (the common part in the nine trans-1,2-diiodoolefin structures) in both the optimized and crystal structures are listed in Table 1. It can be seen that the bond lengths of the C=C in the nine monomers calculated at the B3LYP-D3/6-311++G(d,p) and B3LYP-D3/def2-TZVP levels of theory are all in good agreement with the values seen in the crystal structures. Also, there is only a marginal difference between the C=C bond lengths optimized at the two levels of theory. Therefore, considering the computational cost, the B3LYP-D3/6-311++G(d,p) level of theory was applied to carry out all molecular electrostatic potential ($V_{\mathrm{S,\ max}}$) calculations.

Electrostatic potentials Figure 3 shows contour maps of the electrostatic potential for monomers 1–8. The σ-hole of the two iodine atoms in all nine monomers is positive (see the blue region in Fig. 3). The $V_{\mathrm{S,\ max}}$ values for the two iodine atoms are listed in Table 2. The maximum $V_{\mathrm{S,\ max}}$ value of the nine monomers is 27.30 kJ mol^{-1} for monomer 8. Monomers 5 and 6 had the second and third largest $V_{\mathrm{S,\ max}}$ values of 22.87 kJ mol^{-1} and 22.32 kJ mol^{-1} respectively. The $V_{\mathrm{S,\ max}}$ values for monomers 7(a) and 7(b) are the smallest among all monomers, which are 14.96 kJ mol^{-1} and 15.18 kJ mol^{-1}, respectively. Based on a comparison of all the studied monomers, the iodine atom's chemical environment most strongly affects the electrostatic potential of iodine's σ-hole.

Dimer

Geometries

Six dimers of diiodoalkene were provided in the experimental supplementary data of ref. [41], including dimers 2, 3, 5, 6, 7b, and 8. Each of these dimer structures was partially geometry-optimized at the B3LYP-D3/6-311++G(d,p) and B3LYP-D3/def2-TZVP levels of theory. Because the dimers were too large to be fully geometry-optimized, partial atoms or groups were fixed to ensure optimization is successful, with the fixed atoms or groups chosen to be far away from the locations of the noncovalent bonds (e.g., I…I, I…O, I…C(π), I…H and O…O) formed. The details of fixed atoms or groups for each dimer are listed in the *Supporting Information*. The geometries optimized at the B3LYP-D3/6-311++G(d,p) level of theory are shown in Fig. 4. The noncovalent bond lengths of each dimer, including the values in crystal structures and the values calculated at the B3LYP-D3/6-311++G(d,p) and B3LYP-D3/def2-TZVP levels of theory, are listed in Table 3. The deviations between the crystal structure values and the values calculated at the two levels of theory are quite small. The average deviation between the noncovalent bond lengths optimized at the B3LYP-D3/6-311++G(d,p) level of theory and the values in crystal structures are 0.123 Å, and the corresponding deviation is 0.101 Å between the values optimized at the B3LYP-D3/def2-TZVP levels of theory and the crystal structure values. Again, the noncovalent bond lengths optimized at these two levels of theory are similar. Because the electron charge distribution of the halogen atom is anisotropic, the halogen can act both as the Lewis acid and as the Lewis base [56–59]. This is why dihalogen bonds are possible in the 6 dimers.

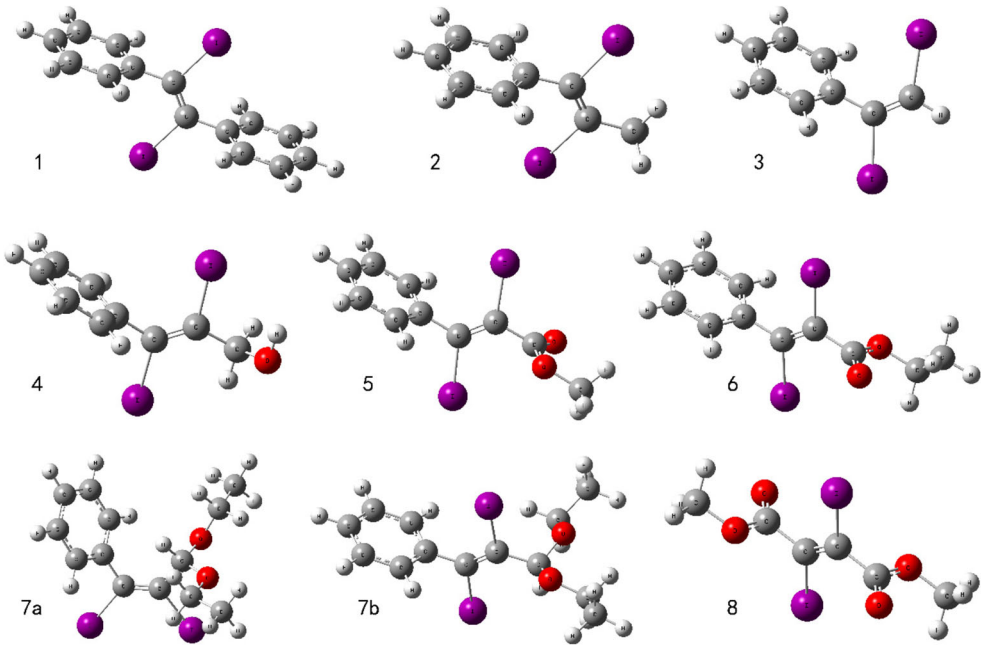

Fig. 2 Overview over the molecular structures of the compounds. The purple atoms stand for I, the red atoms are O, the gray atoms are C, and the white ones are H

Interaction energies

There are five different types of intermolecular noncovalent interactions in the six diiodoalkene dimers (see Fig. 4): I…I, I…O, I…C(π), I…H, and O…O. Interaction energy is an important measure of the strength of an intermolecular interaction. The interaction energy in the dimers can be regarded as the energy difference between the dimer and the monomers as captured via Eq. (1). Table 4 summarizes the interaction energies of the halogen bonds in the six dimers. All results were corrected for BSSE by using counterpoise methods. Naturally, the effect of BSSE correction is prominent for halogen bonds. Calculations are carried out for crystal and optimized dimers, respectively, to explore whether if it is necessary to optimize the crystal structure geometries.

Of all the dimers shown in Fig. 4, dimer 2 possesses the smallest number of intermolecular noncovalent bonds: two halogen bonds of I…I and I…H. Its interaction energies calculated at the B3LYP-D3/6-311++G(d,p) level of theory are − 9.58 kJ mol^{-1} and − 11.67 kJ mol^{-1} respectively for crystal

Table 1 Bond lengths (Å) of C=C in the nine monomers optimized at the B3LYP-D3/6-311++G(d,p) and B3LYP-D3/def2-tzvp levels of theory

Monomer	B3LYP-D3/6-311++G(d,p)	B3LYP-D3/def2-tzvp	Crystal[a]	Abs. dev.1[b]	Abs. dev.2[c]	Abs. dev[d]
1	1.331	1.326	1.291	0.040	0.036	0.004
2	1.330	1.326	1.247	0.083	0.079	0.004
3	1.327	1.323	1.301	0.026	0.022	0.004
4	1.329	1.325	1.333	0.004	0.008	0.004
5	1.328	1.324	1.316	0.012	0.009	0.003
6	1.328	1.324	1.309	0.019	0.016	0.003
7a	1.338	1.334	1.329	0.009	0.005	0.004
7b	1.330	1.326	1.313	0.017	0.013	0.004
8	1.326	1.322	1.323	0.003	0.002	0.004
Average	\	\		0.024	0.021	0.004

[a] From Ref. [29]

[b] The bond length deviations between the values optimized at the B3LYP-D3/6-311++G(d,p) level of theory and the values in the crystal structures

[c] The bond length deviations between the values optimized at the B3LYP-D3/def2-tzvp level of theory and the values in the crystal structures

[d] The bond length deviations between the values optimized at the B3LYP-D3/6-311++G(d,p) and the values optimized at the B3LYP-D3/def2-tzvp level of theory, respectively

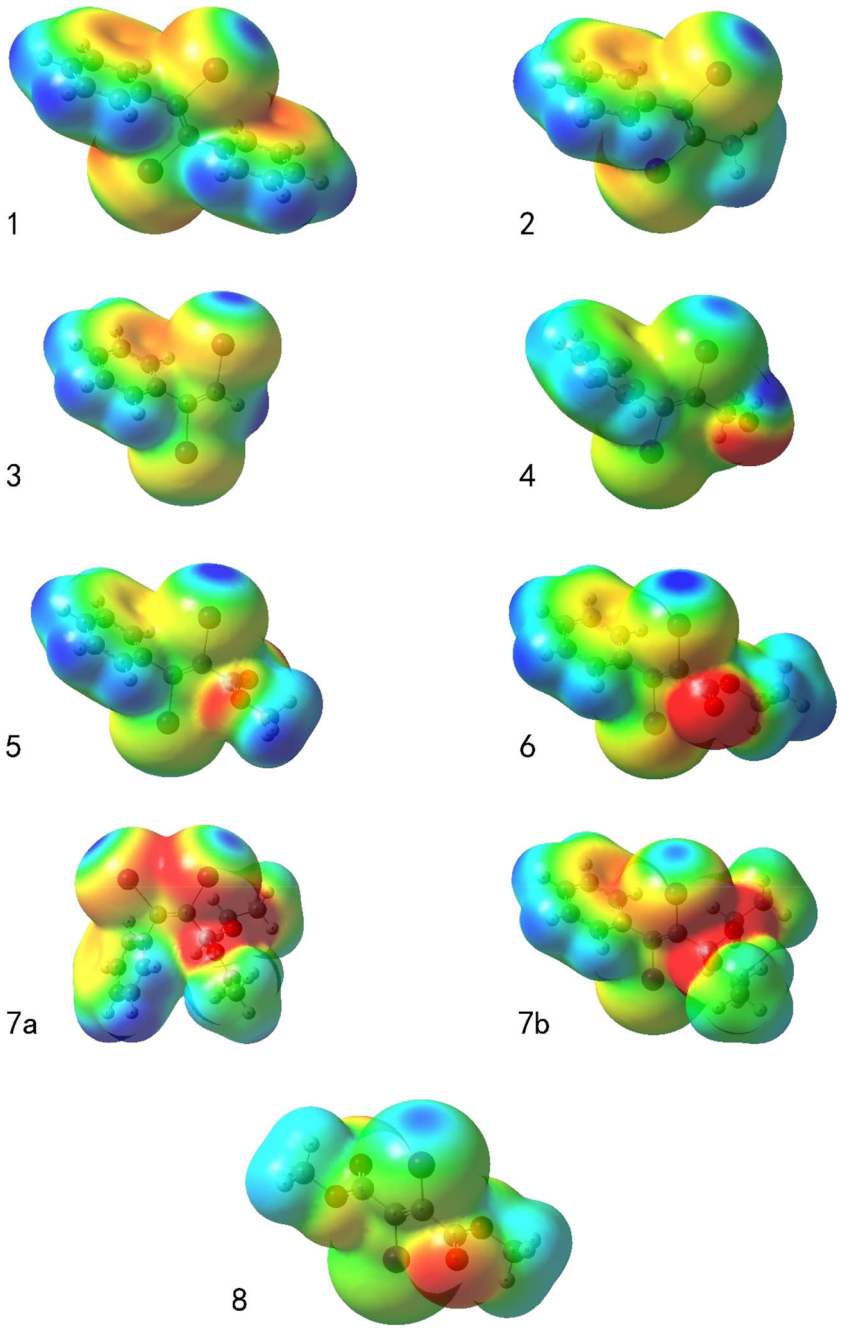

Fig. 3 Electrostatic potentials mapped on the surface of monomer molecules electron density (0.001 e au^{-3}). The electrostatic potential varies from negative (red) to positive (blue)

and optimized geometries; and the respective values are − 11.7 kJ mol^{-1} and − 12.57 kJ mol^{-1} at the B3LYP-D3/def2-TZVP level of theory. Dimer 3 contains three halogen bonds of I…I, I…C(π), I2…C27(π), and I17…C12(π). Dimer 3 has the second highest interaction energy (Table 4) due to the two strong I…C(π) noncovalent bonds. Similarly, the I…C(π) noncovalent bond was also found in dimers 5 and 6; I23…C11(π) in dimer 5 and I1…C33(π) in dimer 6. Moreover, the halogen bond of type I…O was found in dimers 5 (I2…O25) and 6 (I27…O3). The respective interaction energies computed at the two levels of theory are − 29.44 kJ mol^{-1} and − 32.02 kJ mol^{-1} for crystal dimer 5 and − 34.19 kJ mol^{-1} and − 31.79 kJ mol^{-1} for the geometry-optimized dimer 5. Equally, the respective interaction energies computed at the two levels of theory are − 24.59 kJ mol^{-1} and − 26.45 kJ mol^{-1} for crystal dimer 6 and − 29.86 kJ mol^{-1} and − 27.00 kJ mol^{-1} for the optimized dimer. The interaction energy in dimer 7b is also very high because there are five halogen bonds in dimer 7b: one I…I, one I…C(π), and three I…H, the details are shown in Fig. 4 and Table 4. The highest interaction energy occurs in dimer 8, and the corresponding interaction energies computed at the two levels of theory are −

Table 2 The electrostatic potential ($V_{S,\ max}$, kJ mol^{-1}) on iodine atoms in the nine monomers calculated at the B3LYP-D3/6-311++G(d,p) level of theory

Monomer	I_1 ($V_{S,\ max}$)	I_2 ($V_{S,`max}$)
1	16.33	16.30
2	17.27	17.42
3	20.08	19.17
4	21.12	19.83
5	22.87	20.45
6	22.32	20.11
7a	14.96	16.77
7b	15.18	18.81
8	27.30	27.29

I_1 far away from benzene ring

I_2 near benzene ring

36.75 kJ mol^{-1} and − 39.09 kJ mol^{-1}, respectively, for crystal dimer 8, and are − 44.55 kJ mol^{-1} and − 39.95 kJ mol^{-1} for optimized dimer 8. This dimer has three halogen bonds of I…O, I…C(π), and I…H and one O…O noncovalent bond. To summarize, in Table 4, both the interaction energies (E_Int) and the BSSE energies (E_BSSE) for crystal dimers calculated at the two levels of theory are very close to the values for the optimized dimers. Therefore, the properties of halogen bonds can be calculated directly using the crystal structures without geometry optimization.

Natural bond orbital analysis

To better understand the intermolecular interactions, natural bond orbital (NBO) analysis was carried out to characterize the weak interactions. Formation of complexes involving noncovalent bonds is associated with an orbital interaction between the bonding orbital in the electron donor and the antibonding orbital in the electron acceptor. Table 5 lists the second-order perturbation energy ($E^{(2)}$) and the charge transfer (Δq) obtained by NBO analysis. Both $E^{(2)}$ and Δq represent the transfer from one molecule (donor) to the other molecule (acceptor) in the six dimers. Owing to the time-consuming nature of the B3LYP-D3/def2-TZVP level of theory, all NBO calculations were carried out at the B3LYP-D3/6-311++G(d,p) level of theory. The second-order perturbation energy represents the degree of charge transfer from the bonding orbital to the antibonding orbital, which is the degree of electron delocalization. Ultimately, the second-order perturbation energy allows us to quantitatively evaluate the charge transfer due to the formation of the halogen bond.

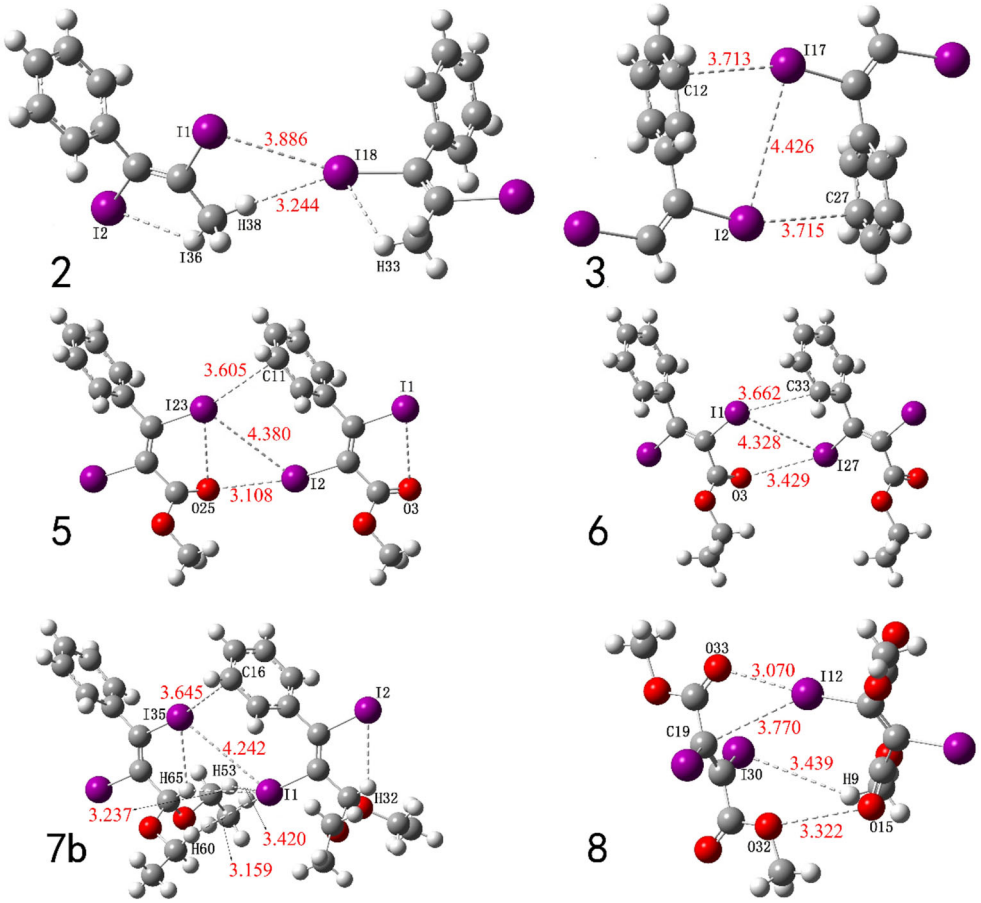

Fig. 4 Organic crystal structures of the dimers concerned with intermolecular interactions given by dotted line

Table 3 Noncovalent bond lengths (Å) in the six dimers optimized at the B3LYP-D3/6-311++G(d,p) and B3LYP-D3/def2-tzvp levels of thery as well as the values in crystal structures

Dimer	Noncovalent bond	B3LYP-D3/6-311++G(d,p)	B3LYP-D3/def2-tzvp	Crystal[a]	Abs. dev. 1[b]	Abs. dev. 2[c]
2	I1…I18	3.886	3.825	3.884	0.002	0.059
	I18…H38	3.244	3.193	3.166	0.078	0.027
3	I2…I17	4.426	4.404	4.486	0.060	0.082
	I2…C27(π)	3.715	3.708	3.573	0.142	0.135
	I17…C12(π)	3.713	3.706	3.573	0.140	0.133
5	I2…I23	4.380	4.174	4.201	0.179	0.027
	I2…O25	3.108	3.314	3.143	0.035	0.171
	I23…C11(π)	3.605	3.529	3.372	0.233	0.157
6	I1…I27	4.328	4.172	4.261	0.067	0.089
	I27…O3	3.429	3.250	3.498	0.069	0.248
	I1…C33(π)	3.662	3.504	3.529	0.133	0.025
7b	I1…I35	4.242	4.247	4.265	0.023	0.018
	I35…C16(π)	3.645	3.688	3.441	0.204	0.247
	I1…H53	3.420	3.456	3.683	0.263	0.227
	I1…H60	3.159	3.150	3.195	0.036	0.045
	I1…H65	3.237	3.249	3.422	0.185	0.173
8	I12…O33	3.070	3.027	3.005	0.065	0.022
	I12…C19(π)	3.770	3.693	3.662	0.108	0.031
	I30…H9	3.639	3.763	3.763	0.124	0.000
	O15…O32	3.322	3.233	3.233	0.089	0.000
Average	\	\		\	0.123	0.101

[a] From Ref. [29]

[b] The halogen bond length deviations between the values optimized at the B3LYP-D3/6-311++G(d,p) level of theory and the values in crystal structures

[c] The halogen bond length deviations between the values optimized at the B3LYP-D3/def2-tzvp level of theory and the values in crystal structures

The results listed in Table 5 show that there is a positive relationship between the second-order perturbation energy $E^{(2)}$ and the charge transfer Δq in the studied systems. Due to the centrosymmetry of dimer 3, the charge transfer from one monomer to another in both the crystal and optimized dimers is zero. Figure 5 presents the strong linear relationship between Δq and $E^{(2)}$ with the exception of 7b. Dimer 7b forms more I…H halogen bonds compared to other dimers. The linear relationship between Δq and $E^{(2)}$ indicates that charge transfer is an important factor in the noncovalent bonds seen in crystal systems.

Table 4 Interaction energies (kJ mol^{-1}) of the six dimers computed at the B3LYP-D3/6–311++G(d,p) and B3LYP-D3/def2-tzvp levels of theory with BSSE energy (kJ mol^{-1})

Dimer	B3LYP-D3/6-311++G(d,p)				B3LYP-D3/def2-tzvp			
	Crystal		Optimized		Crystal[c]		Optimized	
	E_Int	E_BSSE	E_Int	E_BSSE	E_Int	E_BSSE	E_Int	E_BSSE
2	− 9.58	0.94	− 11.67	1.00	− 11.77	0.18	− 12.57	0.17
3	− 30.37	3.27	− 31.04	3.19	− 32.13	0.87	− 32.16	1.20
5	− 29.44	3.06	− 34.19	3.25	− 32.02	1.31	− 31.79	1.22
6	− 24.59	2.65	− 29.86	3.35	− 26.45	0.95	− 27.00	1.30
7b	− 28.12	3.88	− 27.52	3.90	− 30.41	1.40	− 29.86	1.32
8	− 36.75	5.00	− 44.55	5.84	− 39.09	2.10	− 39.95	2.16

Table 5 Natural bond orbital (NBO) analysis at the B3LYP-D3/6-311++G(d,p) level of theory for crystal and optimized dimers

Dimer	Crystal		Optimized at the B3LYP-D3/6-311++G(d,p)	
	$E^{(2)}$	Δq	$E^{(2)}$	Δq
2	11.33	0.022	13.08	0.024
3	0	0	0	0
5	0.67	0.006	0.25	0.001
6	4.38	0.008	5.81	0.005
7b	13.88	0.006	15.80	0.006
8	14.84	0.019	12.24	0.018

Topological properties

The topological and energetic properties at the BCPs of the interactions between the two molecules in the six dimers were analyzed by comparing the following parameters; the electron density ρ(b), the Laplacian of electron density $\nabla^2\rho$(b), the kinetic electron energy density G_b, the potential electron energy density V_b, the sum of G_b and V_b (H_b), and the ratio of G_b to V_b ($-G_b/V_b$). The results are collected in Table 6. A positive value of $\nabla^2\rho$(b) implies an interaction between closed shell complexes; ionic interaction, van der Waals force, or hydrogen bonding, while a negative value of $\nabla^2\rho$(b) indicates a shared interaction as in a covalent bond [60]. Rozas's study [61] concluded that $\nabla^2\rho$(b) and H_b may be useful in characterization of the strength of interactions. This means that for weak A…B interactions, where $\nabla^2\rho(b) > 0$ and $H_b > 0$, the interactions are mainly electrostatic; for medium strength interactions, where$\nabla^2\rho(b) > 0$ and $H_b < 0$, the interactions are partly covalent in nature, while strong interactions show $\nabla^2\rho(b) < 0$ and $H_b < 0$; these are characteristically covalent. Measures of the covalency in noncovalent interactions include the kinetic electron energy density G_c (positive), the potential electron energy density V_c (negative), and the ratio $-G_c/V_c$. Values of $-G_c/V_c > 1$ generally indicate a noncovalent interaction, whereas when $-G_c/V_c$ is < 1, the interaction is covalent in nature. For the dimers investigated here (in Table 6), all $\nabla^2\rho$(b) values are positive, the H_c values are positive, and the $-G_c/V_c$ values are greater than 1. This means that these interactions belong to weak interactions of an electrostatic nature.

The electron density, ρ(b), at the bond critical point is used to describe the strength of a bond, where the larger the value of ρ(b), the stronger the bond. In dimer 2 (see Fig. 5), the intermolecular halogen bond of I1…I18 is the strongest with $\rho(b) = 0.008$ au. In dimer 3, the halogen bonds of I2…C27(π) and I17…C12(π)) were strongest; their ρ(b) was 0.007 au. In dimer 5, the I2…O25 bond was the strongest with a ρ(b) value of 0.01 au. In dimer 6, the I1…C33(π) interaction was the strongest and its ρ(b) was 0.008 au. In dimer 7b, the I35…C16(π) bond was the strongest and its ρ(b) was 0.009 au. In dimer 8, the I12…O33 was the strongest and its ρ(b) was 0.015 au. The results concluded from the topological measures of interaction properties are coincident with the experimental results reported in Table 3.

Figure 6 presents the regions of electronic concentration and depletion along each bond in the six dimers; both the

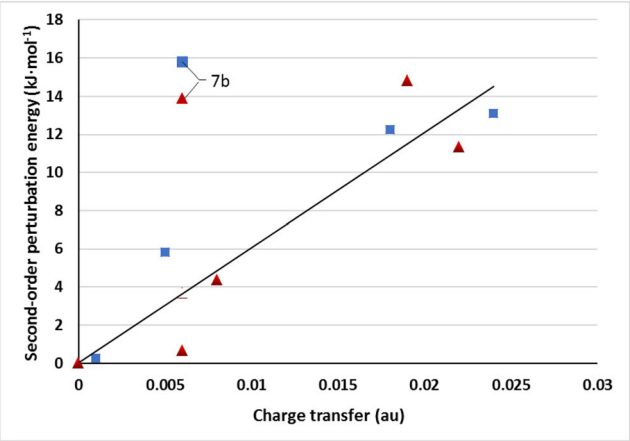

Fig. 5 The charge transfer (au) vs. second-order perturbation energy (kJ mol^{-1})

Table 6 Topological properties (au) of BCPs in the six dimers computed at the B3LYP-D3/6-311++G(d,p) level of theory

Dimer	Bond	ρ(b)	$\nabla^2\rho$(b)	V_b	G_b	H_b	$-G_b/V_b$
2	I1…I18	0.008	0.022	−0.004	0.005	0.001	1.224
	I18…H38	0.006	0.017	−0.003	0.003	0.001	1.255
3	I2…I17	0.003	0.010	−0.001	0.002	0.001	1.422
	I2…C27(π)	0.007	0.021	−0.003	0.004	0.001	1.270
	I17…C12(π)	0.007	0.021	−0.003	0.004	0.001	1.270
5	I2…I23	0.005	0.015	−0.002	0.003	0.001	1.316
	I2…O25	0.010	0.038	−0.007	0.008	0.001	1.184
	I23…C11	0.009	0.026	−0.005	0.006	0.001	1.218
6	I1…I27	0.005	0.013	−0.002	0.003	0.001	1.330
	I1…C33(π)	0.008	0.021	−0.003	0.004	0.001	1.293
	I27…O3	0.006	0.021	−0.004	0.004	0.001	1.204
7b	I1…I35	0.005	0.013	−0.002	0.003	0.001	1.322
	I35…C16(π)	0.009	0.025	−0.004	0.005	0.001	1.279
	I1…H53	0.002	0.007	−0.001	0.001	0.000	1.377
	I1…H60	0.005	0.014	−0.002	0.003	0.001	1.255
	I1…H65	0.003	0.010	−0.002	0.002	0.000	1.276
8	I12…C19(π)	0.006	0.018	−0.003	0.004	0.001	1.268
	I12…O33	0.015	0.048	−0.010	0.011	0.001	1.103
	I30…H9	0.002	0.006	−0.001	0.001	0.000	1.452
	O15…O32	0.004	0.018	−0.003	0.004	0.001	1.212

contour maps (left) and relief maps (right) of $\nabla^2\rho$(b) are shown. The blue points denote BCPs. The blue lines denote positive Laplacian of electron density, which indicate interactions of an ionic character (e.g., van der Waals or intermolecular interactions), and the red lines denote negative Laplacian of electron density which indicate covalent bonds. The corresponding values of the Laplacian of electron density are listed in Table 6. Relief maps provide an intuitive view of the Laplacian of electron density, the curves above the plane show the positive Laplacian of electron density, and the curves below the plane show the negative Laplacian of electron density.

Figure 7 shows the bond lengths of halogen bonds (e.g., I…I, I…O, I…C(π) in Table 3) and their relationship with electron densities ρ(b). For the halogen bonds, the lower the electron density, the longer the bond length. Therefore, the electron density might serve as a rough measure to estimate the strength of halogen bonding interactions.

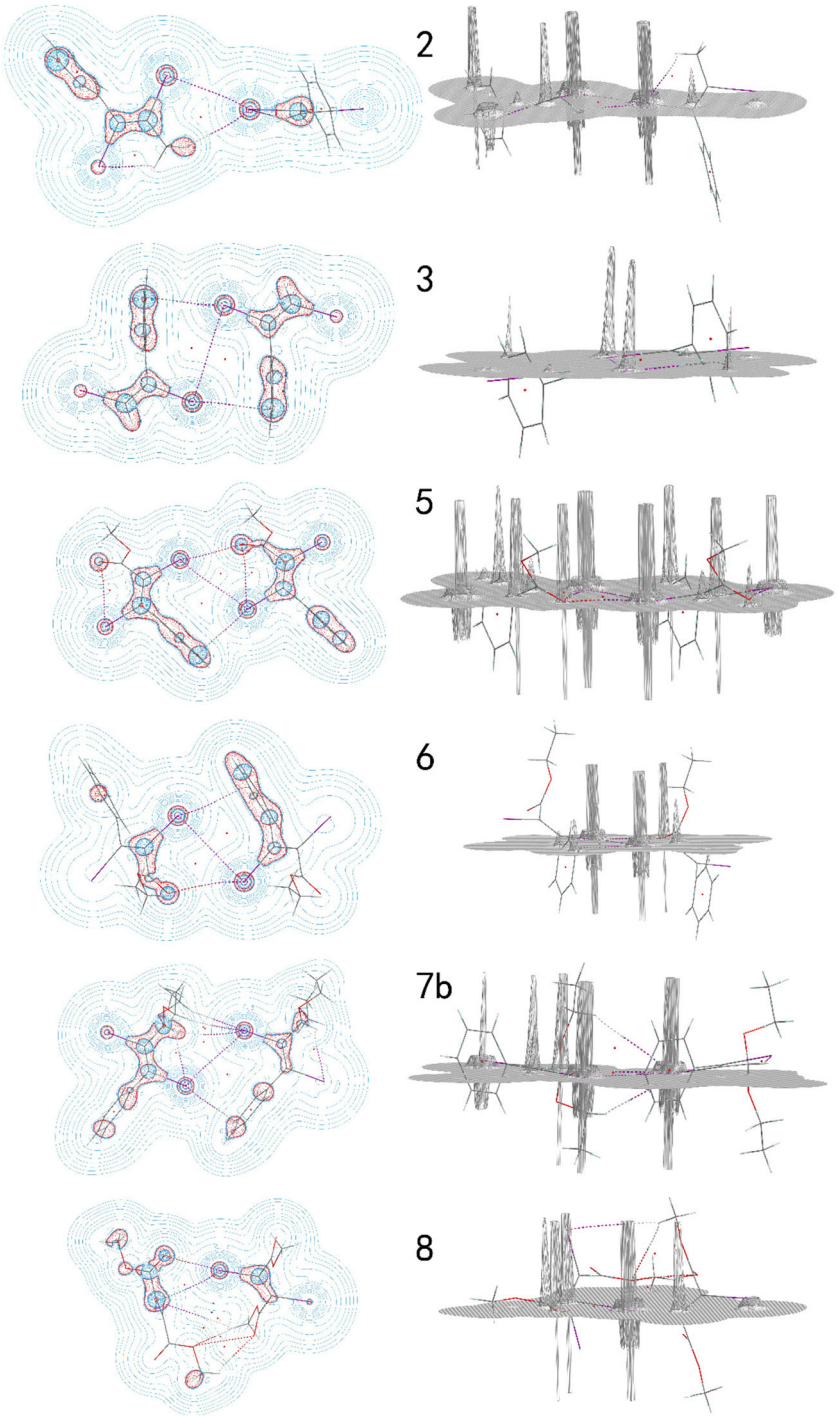

Fig. 6 Molecular contour maps (left) and relief maps (right) of Laplacian of the electron density for the six dimers

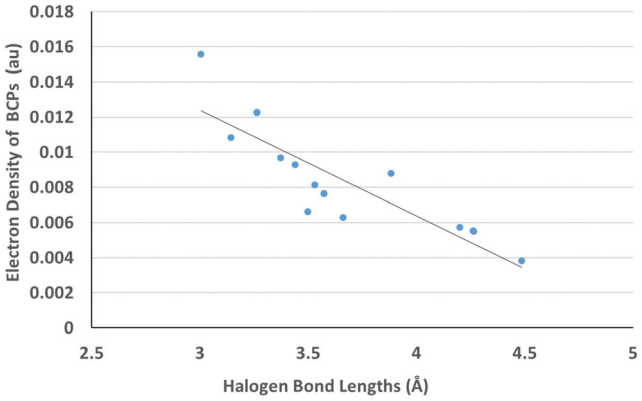

Fig. 7 Relationship between the halogen bonds lengths (Å) and the electron densities at the BCPs (au)

Conclusions

In this study, ab initio and QTAIM studies were performed to explore the nature of halogen bonds and some other noncovalent bonds in a series of crystal structure geometries of trans-1,2-diiodoolefins. The ab initio calculations were carried out at the B3LYP-D3/6-311++G(d,p) and B3LYP-D3/def2-TZVP levels of theory for both crystal and optimized monomers and dimers. Firstly, the calculation results show deviations between the two levels of theory to be quite small. Secondly, the computational values for optimized structures are close to the values for crystal structures.

The reported results provide important information concerning the physical chemistry of these materials. In particular, the crystal geometrical architecture and intermolecular bonding properties were shown to be reproducible with the calculations. The interaction energy and electron density appear to be appropriate tools to judge the stabilities of the crystal structures. Quantification of the noncovalent bonding energy between the molecules in dimers was evaluated both on the crystal and optimized structures, and the interaction energies were within 11.67 kJ mol^{-1} and 44.55 kJ mol^{-1} with B3LYP-D3/6-311++G(d,p). The intermolecular interactions responsible for the formation of the dimers are weak to moderate in strength, these interactions were clearly of enough local significance to guide the solid state crystallization process. Moreover, for the halogen bonds of type I…I, I…O, and I…C(π), there is a strong linear relationship between the electron densities ρ(b) and the bond lengths. This confirms the relationships between electron density and the stability of halogen bonds.

Funding This work was supported by the Fundamental Research Funds for the Central Universities (Grant No. lzujbky-2019-cd05), the National Natural Science Foundation of China (No. 81973786), and the Science Foundation of Guangxi (AA17204096, AD16380076).

References

1. Shing HP (2017) Halogen bonding in medicinal chemistry: from observation to prediction. Future Med Chem 9:637–640
2. Wilcken R, Zimmermann MO, Lange A, Joerger AC, Boeckler FM (2013) Principles and applications of halogen bonding in medicinal chemistry and chemical biology. J Mol Model 56:1363–1388
3. Jungbauer SH, Bulfield D, Kniep F, Lehmann CW, Herdtweck E, Huber SM (2014) Toward molecular recognition: three-point halogen bonding in the solid state and in solution. J Am Chem Soc 136: 16740–16743
4. Parlane FGL, Mustoe C, Kellett CW, Simon SJ, Swords WB, Meyer GJ, Kennepohl P, Berlinguette CP (2017) Spectroscopic detection of halogen bonding resolves dye regeneration in the dye-sensitized solar cell. Nat Commun 8:1761–1768
5. Priimagi A, Cavallo G, Metrangolo P, Resati G (2013) The halogen bond in the design of functional supramolecular materials: recent advances. Acc Chem Res 46:2686–2695
6. Metrangolo P, Resnati G, Pilati T (2008) Halogen bonding in crystal engineering. Struct Bond 126:105–136
7. Raatikainen K, Rissanen K (2012) Breathing molecular crystals: halogen- and hydrogen-bonded porous molecular crystals with solvent induced adaptation of the nanosized channels. Chem Sci 3:1235–1239
8. Mukherjee A, Tothadi S, Gautam R (2014) Desiraju, Halogen bonds in crystal engineering: like hydrogen bonds yet different. Acc Chem Res 47:2514–2524
9. Desiraju GR, Ho PS, Kloo L, Legon AC, Marquardt R, Metrangolo P, Politzer P, Resnati G, Rissanen K (2013) Definition of the halogen bond (IUPAC Recommendations 2013). Pure Appl Chem 85:1711–1713
10. Peter P, Jane SM (2020) Electrostatics and polarization in σ- and π-hole noncovalent interactions: an overview. Chemphyschem 21:579–588
11. Cavallo G, Metrangolo P, Milani R, Pilati T, Priimagi A, Resnati G, Terraneo G (2016) The halogen bond. Chem Rev 116:2478–2601
12. Erdelyi M (2012) Halogen bonding in solution. Chem Soc Rev 41: 3547–3557
13. Parisini E, Metrangolo P, Pilati T, Resnati G, Terraneo G (2011) Halogen bonding in halocarbon-protein complexes: a structural survey. Chem Soc Rev 40:2267–2278
14. Metrangolo, Resnati G (2012) Halogen bonding: where we are and where we are going. Cryst Growth Des 12:5835–5838
15. Carlsson AC, Gräfenstein J, Budnjo A, Laurila JL, Bergquist J, Karim A, Kleinmaier R, Brath U, Erdélyi M (2012) Symmetric halogen bonding is preferred in solution. J Am Chem Soc 134:5706–5715
16. Shuman L, Tianlv X, van Mourik T, Früchtl H, Kirk SR, Jenkins S (2019) Halogen and hydrogen bonding in halogenabenzene/NH3 complexes compared using next-generation QTAIM. Molecules 24:2875–2886
17. Walsh RB, Padgett CW, Metrangolo P (2001) Crsytal engineering through halogen bonding: complexes of nitrogen heterocycles with organic iodides. Cryst Growth Des 1:165–175
18. Siram RBK, Karothu DP, Row TNG, Patil S (2013) Unique type II halogen···halogen interactions in pentafluorophenyl-appended 2, 2′-bithiazoles. Cryst Growth Des 13:1045–1049
19. Grabowski SJ (2013) Hydrogen and halogen bonds are ruled by the same mechanisms. Phys Chem Chem Phys 15:7249–7259
20. Metrangolo P, Resnati G (2008) Halogen versus hydrogen. Science 321:918–919
21. Cinčić D, Friščić T, Jones W (2011) Experimental and database studies of three-centered halogen bonds with bifurcated acceptors present in molecular crystals, cocrystals and salts. Cyst Eng Comm 13:3224–3231
22. Politzer P, Murray JS (2013) Halogen bonding: an interim discussion. Chem Phys Chem 14:278–294

23. Brinck T, Borrfors AN (2019) Electrostatics and polarization determine the strength of the halogen bond: a red card for charge transfer. J Mol Model 25:125–133
24. Clark T, Murray JS, Politzer P (2018) A perspective on quantum mechanics and chemical concepts in describing noncovalent interactions. Phys Chem Chem Phys 20:30076–30082
25. Deepa P, Pandiyan BV, Kolandaivel P, Hobza P (2014) Halogen bonds in crystal TTF derivatives: an ab initio quantum mechanical study. Phys Chem Chem Phys 16:2038–2047
26. Koskinen L, Hirva P, Kalenius E, Jääskeläinen S, Rissanen K, Haukka M (2015) Halogen bonds with coordinative nature: halogen bonding in a S–I+–S iodonium complex. Cryst Eng Comm 17:1231–1236
27. Bader RFW (1991) A quantum theory of molecular structure and its applications. Chem Rev 91:893–928
28. Foroutan-Nejad C, Shahbazian S, Marek R (2014) Toward a consistent interpretation of the QTAIM: tortuous link between chemical bonds, interactions, and bond/line paths. Chem Eur J 20:10140–10152
29. Grimme S, Muck-Lichtenfeld C, Erker G, Kehr G, Wang H, Beckers H, Willner H (2009) When do interacting atoms form a chemical bond? Spectroscopic measurements and theoretical analyses of dideuteriophenanthrene. Angew Chem Int Ed 48:2592–2595
30. Spackman MA (2015) How reliable are intermolecular interaction energies estimated from topological analysis of experimental electron densities? Cryst Growth Des 15:5624–5628
31. Politzer P, Murray JS (2019) A looking at bonds and bonding. Struct Chem 30:1153–1157
32. Clark T, Hennemann M, Murray JS, Politzer P (2007) Halogen bonding: the σ-hole. J Mol Model 13:291–296
33. Politzer P, Lane P, Concha MC, Ma Y, Murray JS (2007) An overview of halogen bonding. J Mol Model 13:305–311
34. Zeng Y, Zhang X, Li X, Zheng S, Meng L (2010) Ab initio and AIM studies on typical π-type and pseudo-π-type halogen bonds: comparison with hydrogen bonds. Int J Quantum Chem 111:3725–3740
35. Zhang X, Zeng Y, Li X, Meng L, Zheng S (2011) A computational study on the nature of the halogen bond between sulfides and dihalogen molecules. Struct Chem 22:567–576
36. Grabowski SJ (2012) QTAIM characteristics of halogen bond and related interactions. J Phys Chem A 116:1838–1845
37. Bauzá A, Seth SK, Frontera A (2018) Molecular electrostatic potential and "atoms-in-molecules" analyses of the interplay between π-hole and lone pair···π/X–H···π/metal···π interactions. J Comput Chem 39:458–463
38. Roselló Y, Benito M, Molins E, Barceló-Oliver M, Frontera A (2019) Adenine as a halogen bond acceptor: a combined experimental and DFT study. Crystals 9:224–233
39. Wzgarda-Raj K, Rybarczyk-Pirek AJ, Wojtulewski S, Palusiak M (2020) C—Br··· S halogen bonds in novel thiourea N-oxide cocrystals: analysis of energetic and QTAIM parameters. Acta Crystallogr C 76:170–176
40. Domagała M, Lutynska A, Palusiak M (2018) Extremely strong halogen bond. The case of a double-charge-assisted halogen bridge. J Phys Chem A 122:5484–5492
41. Hettstedt C, Mayer P, Karaghiosoff K (2015) Halogen bonding in the crystal structures of 1,2-diiodo alkenes. New J Chem 39:8522–8533
42. Weigend F, Ahlrichs R (2005) Balanced basis sets of split valence, triple zeta valence and quadruple zeta valence quality for H to Rn: design and assessment of accuracy. Phys Chem Chem Phys 7:3297–3305
43. Grimme S, Antony J, Ehrlich S, Krieg H (2010) A consistent and accurate ab initio parametrization of density functional dispersion correction (DFT-D) for the 94 elements H-Pu. J Chem Phys 132: 154104–154123
44. Grimme S, Ehilich S, Goerigk L (2011) Effect of the damping function in dispersion corrected density functional theory. J Comput Chem 32:1456–1465
45. Frisch MJ, Truchs GW, Schlegel HB, Scuseria GE, Robb MA, Cheeseman JR, Schmani G, Barone V, Mennucci B, Petersson GA, Nakatsuji H, Caricato M, Li X, Hratchian HP, Izmaylov AF, Bloino J, Zheng G, Sonnenberg JL, Hada M, Ehara M, Toyota K, Fukuda R, Hasegawa J, Ishida M, Nakajima T, Honda Y, Kitao O, Nakai H, Vreven T, Montgomery JJA, Peralta JE, Ogliaro F, Bearpark M, Heyd JJ, Brothers E, Kudin KN, Staroverov VN, Kobayashi R, Normand J, Raghavachari K, Rendell A, Burant JC, Iyengar SS, Tomasi J, Cossi M, Rega N, Millam NJ, Klene M, Knox JE, Cross JB, Bakken V, Adamo C, Jaramillo J, Gomperts R, Stratmann RE, Yazyev O, Austin AJ, Cammi R, Pomelli C, Ochterski JW, Martin RL, Morokuma K, Zakrzewski VG, Voth GA, Salvador P, Dannenberg JJ, Dapprich S, Daniels AD, Farkas Ö, Foresman JB, Ortiz JV, Cioslowski J, Fox DJ (2015) Gaussian 09, Revision E.01. Gaussian, Inc., Wallingford, CT
46. Zhao H, Chang J, Du L (2016) Effect of hydrogen bonding on the spectroscopic properties of molecular complexes with aromatic rings as acceptors. Comput Theor Chem 1084:126–132
47. Zhang Q, Du L (2016) Hydrogen bonding in the carboxylic acid–aldehyde complexes. Comput Theor Chem 1078:123–128
48. Tang S, Zhao H, Du L (2016) Hydrogen bonding in alcohol–ethylene oxide and alcohol–ethylene sulfide complexes. RSC Adv 6:91233–91242
49. Bauzá A, Quinonero D, Deya PM, Frontera A (2013) Halogen bonding versus chalcogen and pnicogen bonding: a combined Cambridge structural database and theoretical study. Cryst Eng Comm 15:3137–3144
50. Kolář M, Hostaš J, Hobza P (2014) The strength and directionality of a halogen bond are co-determined by the magnitude and size of the σ-hole. Phys Chem Chem Phys 16:9987–9996
51. Bauzá A, Ramis R, Frontera A (2014) Computational study of anion recognition based on tetrel and hydrogen bonding interaction by calix[4]pyrrole derivatives. Comput Theor Chem 1038:67–70
52. Boys SF, Bernardi F (1970) The calculation of small molecular interactions by the differences of separate total energies. Some procedures with reduced errors. Mol Phys 19:553–566
53. Bader RFW, Carroll MT, Cheeseman JR, Cheng C (1987) Properties of atoms in molecules: atomic volumes. J Am Chem Soc 109:7968–7979
54. Glendening ED, Reed AE, Carpenter JE, Weinhold F (1990) NBO 3.1, QCPE Bull 1990, 10, 58
55. Keith TA (2011) AIMAll, 15.09.27, TK Gristmill Software
56. Zordan F, Brammer L, Sherwood P (2005) Supramolecular chemistry of halogens: complementary features of inorganic (M− X) and organic (C− X ') halogens applied to M− X...X '− C halogen bond formation. J Am Chem Soc 127:5979–5989
57. Domagała M, Matczak P, Palusiak M (2012) Halogen bond, hydrogen bond and N··· C interaction–on interrelation among these three noncovalent interactions. Comput Theor Chem 998:26–33
58. Domagała M, Palusiak M (2014) The influence of substituent effect on noncovalent interactions in ternary complexes stabilized by hydrogen-bonding and halogen-bonding. Comput Theor Chem 1027:173–178
59. Domagała M, Lutyńska A, Palusiak M (2017) Halogen bond versus hydrogen bond: the many-body interactions approach. Int J Quantum Chem 117:e25348–e25356
60. Popelier PLA (2000) Atoms in molecules: an introduction. Prentice Hall, Pearson Education Limited, New York
61. Rozas I, Alkorta I, Elguero J (2000) Behaviour of ylides containing N, O and C atoms as hydrogen bond acceptors. J Am Chem Soc 122:11154–11161